frontiers | Frontiers in Energy Research

TYPE Original Research
PUBLISHED 16 September 2024
DOI 10.3389/fenrg.2024.1472503

OPEN ACCESS

EDITED BY
Zhengmao Li,
Aalto University, Finland

REVIEWED BY
Xiang Gao,
Xi'an University of Technology, China
Ming-Feng Ge,
China University of Geosciences
Wuhan, China
Wentao Jiang,
Northwestern Polytechnical University, China

*CORRESPONDENCE
Guangyu Song,
songgy_1@126.com

RECEIVED 29 July 2024
ACCEPTED 29 August 2024
PUBLISHED 16 September 2024

CITATION
Mei Y, Xu J, Peng C, Kong W, Peng G and Song G (2024) Voltage quality enhancement of distribution network based on unified power quality conditioner with BESS.
Front. Energy Res. 12:1472503.
doi: 10.3389/fenrg.2024.1472503

Voltage quality enhancement of distribution network based on unified power quality conditioner with BESS

Yan Mei, Jiangbo Xu, Chen Peng, Weikang Kong, Gang Peng and Guangyu Song*

Electric Power Research Institute of State Grid Xizang Electric Power Co., Ltd., Lhasa, China

This article proposes a voltage compensation control strategy for the distribution network based on the unified power quality conditioner (UPQC) with battery energy storage systems (BESS) to achieve comprehensive management of the power quality and improve the system dynamic responses. Specifically, aiming at that amplitude and phase jump of the terminal voltage, a capacity configuration compensation scheme is proposed to achieve voltage vector compensation. The series converter is designed to compensate for the amplitude and phase of the load voltage. The parallel converter is designed to realize power compensation and ensure that the grid voltage and current are sinusoidal and in phase. A voltage control approach based on the nonlinear disturbance observer (NDO) is developed for BESS to stabilize the DC bus voltage and improve the anti-interference performance of the current. An NDO is designed to accomplish current disturbance tracking and provide disturbance feedforward compensation. Simulations validate that the proposed approach is effective and feasible.

KEYWORDS

distribution network, power quality, unified power quality conditioner, battery energy storage systems, nonlinear disturbance observer

1 Introduction

WITH the access to distributed energy and the surge of nonlinear loads, the power quality problem of low-voltage distribution network terminals has become increasingly prominent (Mahela et al., 2020). Since power systems become more complex and the demand for electricity continues to grow, maintaining high power quality in distribution networks becomes increasingly challenging. The increasing penetration of renewable energy sources (RES) like solar and wind into the distribution network introduces variability and intermittency, which can further exacerbate power quality problems (Ray et al., 2022). Moreover, the access of nonlinear loads produces a lot of harmonic and reactive power to the distribution network, resulting in voltage distortion, three-phase unbalance, and harmonic pollution. Even it will threaten the safe and stable operation of the grid and cause huge economic losses (Lou et al., 2021; Li et al., 2023). The improvement of power quality in distribution networks has attracted extensive attention of experts from all over the world (Carreno et al., 2024; Li et al., 2024). Due to its diversity in power quality functions, the unified power quality conditioner (UPQC) has become an essential power quality regulation device (Bacon et al., 2022). Combining the advantages of the shunt active power filter and

the series active power filter, the UPQC can compensate for power supply voltage, eliminate harmonic current, and realize reactive power compensation (Wang J. et al., 2021).

With the rapid rise of the UPQC, a great deal of theoretical research and engineering practice has been carried out (da Silva et al., 2020; Yang and Jin, 2021; Khosravi et al., 2023; Sanjenbam et al., 2023). Dash and Ray (2021) designed a novel photovoltaic-based UPQC topology and proposed an adaptive control approach to eliminate current distortion and improve system robustness. However, the randomness of photovoltaics is not conducive to the DC voltage stability and will result in power fluctuation. Abdalaal and Ho (2022) proposed an enhanced control scheme without additional sensors to provide reactive power compensation and achieve grid voltage regulation. Xu et al. (2023) presented a dynamic harmonics compensation control strategy for single-phase UPQC to suppress grid voltage harmonics and maintain voltage stabilization. A distributed parallel control scheme of UPQC for the low-voltage distribution network was developed to support the grid voltage and improve the voltage quality of the load in Abdalaal and Ho (2021). Silva et al. (2024) designed a feed-forward control method to accelerate the voltage and current response compensated by UPQC. However, when there are disturbances in the grid, the system cannot obtain an accurate current reference to ensure that the sinusoidal current is not distorted. The structure of the three-phase UPQC was improved to realize the compensation of grid voltage drop and the power factor improvement in Cardoso et al. (2024). This converter does not need the participation of the line-frequency transformer, but the design may require to be simplified. Felinto et al. (2022) developed an improved UPQC in combination with the high-frequency transformer to compensate for load unbalance. The proposed approach requires no control of the DC-DC converter, but it increases the hardware cost and power density. In (Jin et al., 2020), a comprehensive control method for UPQC based on $dq0$-axis detection was proposed to improve the control effect of the conditioner. However, there are significant fluctuations in DC bus voltage and the reactive power compensation effect is not ideal.

To suppress voltage fluctuation and provide power support, the energy storage systems (ESS) in the distribution network have been investigated and implemented (Hosseini and Parvania, 2023; Song et al., 2024a; Tziovani et al., 2022). By integrating UPQC with battery energy storage systems (BESS), it becomes possible to enhance the dynamic response of the system, providing rapid compensation during transient events and contributing to overall grid stability (Charalambous et al., 2021; Zhang et al., 2024). A triple-port active bridge UPQC is designed based on the BESS to improve the fault ride-through performance of the DC grid in Yang R. H. et al. (2022). However, it is less effective in improving power quality in the distribution network. Wang H. et al. (2022) proposed an optimal mitigation scheme by combining fixed energy storage equipment and mobile energy storage equipment to attenuate voltage imbalance and mitigate power fluctuation. Monteiro et al. (2024) utilized the charge and discharge characteristics of the BESS and proposed a new multi-objective UPQC to cope with the power quality issues, which compensates for the grid voltage and load current. Combined with superconducting energy storage, Yang R. et al. (2022) proposed a UPQC based on dual active bridge topology to adjust the terminal voltage and current, which has a simple structure and good voltage stabilization capability. By applying ESS to UPQC, an effective compensation control strategy was developed to achieve voltage recovery and current quality regulation in Çelik and Ahmed (2023). However, the scheme increases the cost investment, and the controller design needs to be further optimized. Somayajula and Crow (2014) proposed an ultracapacitor-based UPQC to mitigate distribution network intermittency and enhance grid power quality. However, the stability and smoothness of the DC voltage is not adequately considered. Devassy and Singh (2021) proposed an automatic transition scheme by integrating photovoltaic and ESS into the UPQC to achieve a continuous and smooth power supply to the load.

In this article, a UPQC-based voltage compensation control strategy for distribution networks is proposed to compensate for the load voltage vector and accomplish system power balance. The main contributions of the article are summarized as follows.

1) A capacity configuration compensation scheme for the distribution network is proposed, which achieves the comprehensive compensation of load voltage and improves the output quality of voltage and current. Compared with other approaches (Bacon et al., 2022; Khosravi et al., 2023; Jin et al., 2020), the proposed scheme compensates for the sudden changes of the load voltage amplitude and phase angle.
2) An NDO-based voltage control approach is developed for BESS to guarantee the stability of DC bus voltage while achieving the bus voltage reference tracking. Unlike other control models (Ray et al., 2022; Sanjenbam et al., 2023; Dash and Ray, 2021), the proposed approach accomplishes disturbance compensation and improves the current waveform quality.
3) The nonlinear disturbance observer (NDO) is developed to achieve disturbance tracking and improve the anti-interference ability of the system, which suppresses the impact of current disturbance on DC voltage stability.

The remainder of the article is organized as follows. Section 2 gives the structure of UPQC. The voltage compensation control strategy of the distribution network based on UPQC is proposed in Section 3. Section 4 shows the simulation results of the proposed strategy. Finally, the conclusion is given in Section 5.

2 System description

The structure of the UPQC mainly includes the series converter, shunt converter, DC bus capacitor, and BESS, as depicted in Figure 1. When the power supply voltage drops, the series converter is regarded as a voltage source to compensate for the grid voltage vector and ensure the voltage quality at the user side, which is connected in series to the distribution network through inductive filtering. The shunt converter is regarded as a current source, which is connected in parallel to the load side through inductive filtering, to compensate for reactive power, eliminate current harmonics, and ensure the sinusoidal characteristics of the grid current. The BESS is used to maintain DC bus voltage stability and provide load power compensation when necessary.

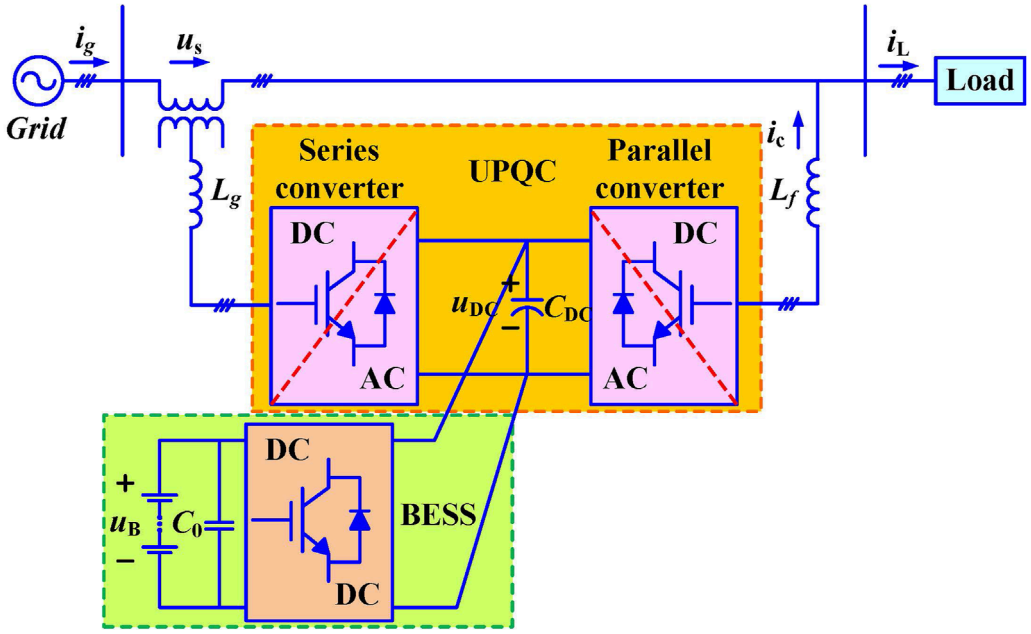

FIGURE 1
Structure diagram of UPQC with BESS.

Based on Kirchhoff's law, the mathematical model of the UPQC is established as

$$\begin{cases} u_{i1} - L_g \dfrac{di_{L_g}}{dt} = u_s \\ u_{i2} - L_f \dfrac{di_c}{dt} = u_L \end{cases} \tag{1}$$

where u_{i1} and u_{i2} represent the output voltages of series converter and shunt converter, respectively, L_g and L_f represent the inductor filters of the series converter and shunt converter, respectively, i_{L_g} and i_c represent the output current of series converter and the compensation current of shunt converter, respectively, u_s represents the compensation voltage of series converter, u_L is load voltage.

Using the coordinate transformation matrix $\widetilde{T}_{dq0}$ (Song et al., 2024a), the UPQC model in dq coordinates can be obtained as

$$\begin{cases} u_{i1dq} - L_g \dfrac{di_{L_g dq}}{dt} + L_g \begin{bmatrix} 0 & \omega & 0 \\ -\omega & 0 & 0 \\ 0 & 0 & 0 \end{bmatrix} i_{L_g dq} = u_{sdq} \\ u_{i2dq} - L_f \dfrac{di_{cdq}}{dt} + L_f \begin{bmatrix} 0 & \omega & 0 \\ -\omega & 0 & 0 \\ 0 & 0 & 0 \end{bmatrix} i_{cdq} = u_{Ldq} \end{cases} \tag{2}$$

where

$$\widetilde{T}_{dq0} = \frac{2}{3} \begin{bmatrix} \cos\varphi & \cos\left(\varphi - \frac{2\pi}{3}\right) & \cos\left(\varphi + \frac{2\pi}{3}\right) \\ \sin\varphi & \sin\left(\varphi - \frac{2\pi}{3}\right) & \sin\left(\varphi + \frac{2\pi}{3}\right) \\ \frac{1}{2} & \frac{1}{2} & \frac{1}{2} \end{bmatrix},$$

subscripts d and q represent dq-axis components of voltage and current, respectively.

Considering the continuous conduction of the switch tube, the BESS model can be constructed as (Song et al., 2024b)

$$\begin{cases} u_B - L_B \dfrac{di_L}{dt} = \left(1 - d_j\right) u_{DC} \\ i_o + C_{DC} \dfrac{du_{DC}}{dt} = \left(1 - d_j\right) i_L \end{cases} \tag{3}$$

where u_B is the battery voltage, i_L is the inductor current, L_B and C_{DC} are the inductor and capacitor of the BESS, i_o and u_{DC} are the output current and output voltage of the BESS, d_j is the control input.

3 Proposed control strategy design

In this section, a voltage compensation control strategy for the distribution network is proposed to achieve comprehensive management of power quality. To address the problem of the voltage jump, a capacity configuration compensation scheme is designed for UPQC to compensate for the amplitude and phase of the load voltage. Then, an NDO-based voltage control approach for BESS is proposed to guarantee the stability of DC bus voltage and suppress voltage fluctuation, where the designed NDO improves the disturbance rejection ability of the system.

3.1 Voltage phasor compensation

Figure 2 displays the voltage and current phasor diagram of the UPQC. In Figure 2, $\dot{u}_g$ denotes the grid voltage, $\dot{i}_g$ and $\dot{i}_L$ denote the grid current and the load current compensated by the UPQC respectively, $\dot{u}_g^{\wedge}$, $\dot{u}_L^{\wedge}$, and $\dot{u}_s^{\wedge}$ denote the grid voltage, the load voltage, and the compensation voltage of series converter when the grid

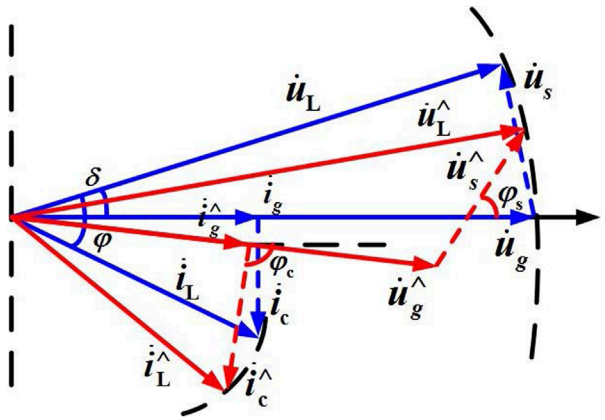

FIGURE 2
Voltage and current phasor diagram of UPQC.

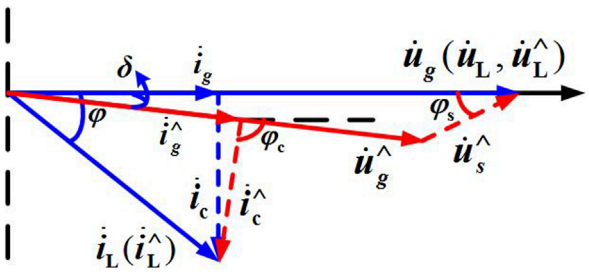

FIGURE 3
Phasor diagram after voltage and current compensation.

voltage drops, respectively, $\dot{i}_g^{\wedge}$, $\dot{i}_L^{\wedge}$, and $\dot{i}_c^{\wedge}$ denote the grid current, the load current, and the compensation current of shunt converter when the supply voltage drops, respectively, δ and φ denote the power angle and impedance angle respectively, φ_s and φ_c denote the phase angles of compensation voltage and compensation current respectively.

When the power grid is operating normally, the load voltage can be denoted as

$$u_L \angle\delta = u_g \angle 0 + u_s \angle\varphi_s \tag{4}$$

Then, the voltage amplitude of the series converter can be obtained as

$$u_s = \sqrt{u_g^2 + u_L^2 - 2u_g u_L \cos\delta} \tag{5}$$

According to the cosine theorem, the voltage phase angle of the series converter can be deduced as

$$\varphi_s = \pi - \arctan\frac{\sin\delta}{1-\cos\delta} \tag{6}$$

To satisfy the power demand of the load, considering the load $S_L = P_L + jQ_L$, the load current can be calculated as

$$i_L \angle(\delta - \phi) = \frac{P_L - jQ_L}{u_L \angle -\delta} \tag{7}$$

Further, to guarantee that the grid current is in phase with the grid voltage, we have

$$i_g = i_L \cos(\delta - \phi) = \frac{\sqrt{P_L^2 + Q_L^2}}{u_L}\cos\left[\arctan\left(\frac{-Q_L}{P_L}\right) + \delta\right] \tag{8}$$

The capacity of the series converter can be configured as

$$S_s = \dot{u}_s \dot{i}_g^{*} = \frac{u_s\sqrt{P_L^2 + Q_L^2}}{u_L}\cos\left[\arctan\left(\frac{-Q_L}{P_L}\right) + \delta\right] \angle\varphi_s \tag{9}$$

Similarly, the capacity of the shunt converter can be configured as

$$S_c = \dot{u}_L \dot{i}_c^{*} = \sqrt{P_L^2 + Q_L^2}\sin\left[\arctan\left(\frac{-Q_L}{P_L}\right) + \delta\right] \angle(\delta + \pi) \tag{10}$$

When the grid voltage sags in amplitude and jumps in phase, the UPQC with BESS injects compensation voltage into the grid and provides compensation current to the load, which improves the load voltage quality and provides active power support and reactive compensation. The phasor diagram after voltage and current compensation is depicted in Figure 3. Based on Kirchhoff's law, the voltage relationship is given as

$$u_L^{\wedge} \angle 0 = u_g^{\wedge} \angle -\delta + u_s^{\wedge} \angle\varphi_s \tag{11}$$

Since the load voltage and current remain constant before and after the grid voltage drops, the following equation holds.

$$i_c^{\wedge} = i_L^{\wedge}\sin\varphi = \frac{\sqrt{P_L^2 + Q_L^2}}{u_L}\sin\left[\arctan\left(\frac{-Q_L}{P_L}\right)\right] \tag{12}$$

According to the sine theorem, the following relation can be obtained as

$$\frac{i_L^{\wedge}}{\sin(\pi - \varphi_c + \delta)} = \frac{i_c^{\wedge}}{\sin(\varphi - \delta)} \tag{13}$$

Further, we have

$$\varphi_c = \pi + \delta - \arcsin\left[\frac{\sin(\varphi - \delta)}{\sin\varphi}\right] \tag{14}$$

The capacity of the shunt converter when voltage phasor attenuation is encounter, is configured as

$$S_c = \dot{u}_L^{\wedge}\dot{i}_c^{\wedge *} = \sqrt{P_L^2 + Q_L^2}\sin\left[\arctan\left(\frac{-Q_L}{P_L}\right)\right] \angle -\varphi_c \tag{15}$$

Likewise, the capacity of the series converter is configured as

$$S_s = \dot{u}_s^{\wedge}\dot{i}_g^{\wedge *} = u_s^{\wedge}\sqrt{i_c^{\wedge 2} + i_L^{\wedge 2} - 2i_c^{\wedge} i_L^{\wedge}\cos(\varphi_c - \varphi)} \angle(\varphi_s - \varphi_c) \tag{16}$$

where $u_s^{\wedge} = \sqrt{u_g^{\wedge 2} + u_L^{\wedge 2} - 2u_g^{\wedge 2}u_L^{\wedge 2}\cos\delta}$, $i_L^{\wedge} = \frac{\sqrt{P_L^2+Q_L^2}}{u_L^{\wedge}}\cos[\arctan(\frac{-Q_L}{P_L})]$.

When there is a fault in the grid and the connection is interrupted, the power required by the load should be provided by BESS. To ensure uninterrupted power supply to the load, the capacity of the BESS is designed as

$$S_B = \frac{P_L t}{\kappa \cdot u_{DC} \cdot \eta_b} \tag{17}$$

where t is the continuous power supply time, κ is the power coefficient, η_b is the charging and discharging efficiency.

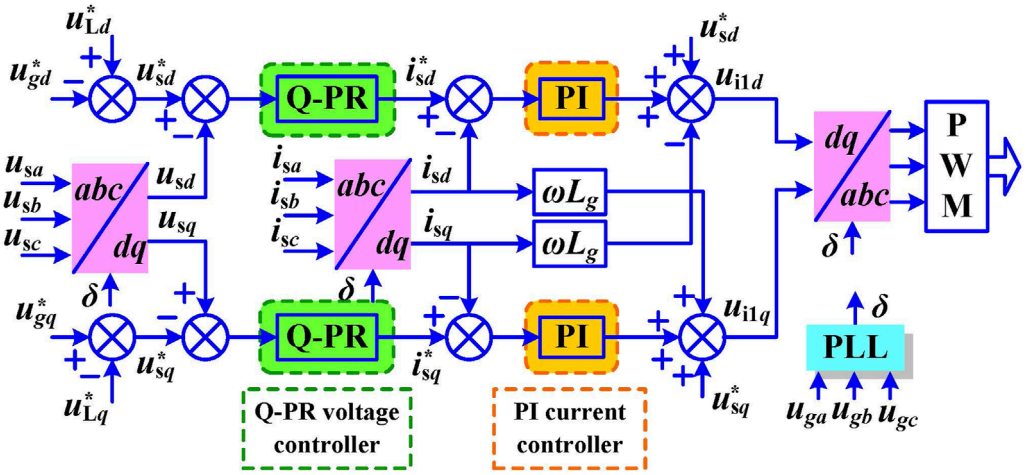

FIGURE 4
Control strategy of series converter.

It can be seen that the proposed compensation scheme realizes the comprehensive compensation of the load voltage vector. When the grid voltage sags, the increase of the shunt compensation current reduces the grid current, which reduces the risk of over-current in the distribution network.

3.2 UPQC control strategy design

In the distribution network, the grid current and load voltage are controllable. In this paper, the voltage compensation control strategy is developed for the UPQC, where the series converter compensates for the grid voltage and the shunt converter compensates for the reactive power of the load, suppresses harmonic current, and ensures the sinusoidal in-phase property between the grid current and grid voltage.

Due to the energy loss and other disturbance factors in the line, the power quality of the load cannot be guaranteed. Especially when encountering faults, the voltage quality of the load will be seriously degraded. To improve the voltage quality of the grid, the control strategy of the series converter is proposed, which is illustrated in Figure 4. It can be noted that compared with other control methods (da Silva et al., 2020; Silva et al., 2024; Jin et al., 2020), the compensation voltage reference u_s^* is generated by the deviation between the grid reference voltage and the load reference voltage (u_L^*, u_g^*), rather than directly using the grid voltage reference. The compensation signal can track its reference to achieve full compensation of the voltage vector. The compensation voltage reference is expressed as

$$\begin{bmatrix} u_{sd}^* \\ u_{sq}^* \end{bmatrix} = \begin{bmatrix} u_{Ld}^* - u_{gd}^* \\ u_{Lq}^* - u_{gq}^* \end{bmatrix} \tag{18}$$

Since the PI controller cannot realize the static error-free tracking for AC component, the quasi-proportional resonant (Q-PR) controllers are employed to achieve voltage tracking without static error and suppress the resonant voltage disturbance. The fundamental frequency current can also realize its reference tracking. The transfer function of the Q-PR controller is expressed as (Song et al., 2024a)

$$G_{\text{Q-PR}}(s) = k_g + \frac{2k_{gr}\omega_r s}{s^2 + 2\omega_r s + \omega_0^2} \tag{19}$$

where k_g and k_{gr} are proportion and resonance gains of Q-PR control, ω_r and ω_0 are cut-off frequency and resonant bandwidth. ω_0 is selected as 628 rad/s to suppress the double-frequency component. Considering the national standard of the frequency fluctuation, ω_r is calculated as 3.14 rad/s.

To stabilize the sinusoidal grid voltage and compensate for the voltage drop, the voltage control law of the series converter is given as

$$\begin{cases} i_{sd}^* = \left(k_g + \dfrac{2k_{gr}\omega_r s}{s^2 + 2\omega_r s + \omega_0^2}\right)\left(u_{sd}^* - u_{sd}\right) \\ i_{sq}^* = \left(k_g + \dfrac{2k_{gr}\omega_r s}{s^2 + 2\omega_r s + \omega_0^2}\right)\left(u_{sq}^* - u_{sq}\right) \end{cases} \tag{20}$$

where i_{sd}^*, i_{sq}^* are the output current reference of the series converter.

To better achieve voltage control and decouple inductor of the series converter, the compensation voltage reference is fed forward to the current control loop. The current control law of the series converter is given as

$$\begin{cases} u_{i1d} = \left(k_{ip} + \dfrac{k_{ii}}{s}\right)\left(i_{sd}^* - i_{sd}\right) - \omega L_g i_{sq} + u_{sd}^* \\ u_{i1q} = \left(k_{ip} + \dfrac{k_{ii}}{s}\right)\left(i_{sq}^* - i_{sq}\right) + \omega L_g i_{sd} + u_{sq}^* \end{cases} \tag{21}$$

where k_{ip}, k_{ii} are the proportional and integral gains of the PI controller.

The control strategy of the shunt converter is illustrated in Figure 5. The DC components of the three-phase load current, grid current and compensation current can be obtained by Park transformation. Since the grid current has both fundamental and harmonic components, the low-pass filter (LPF) is adopted

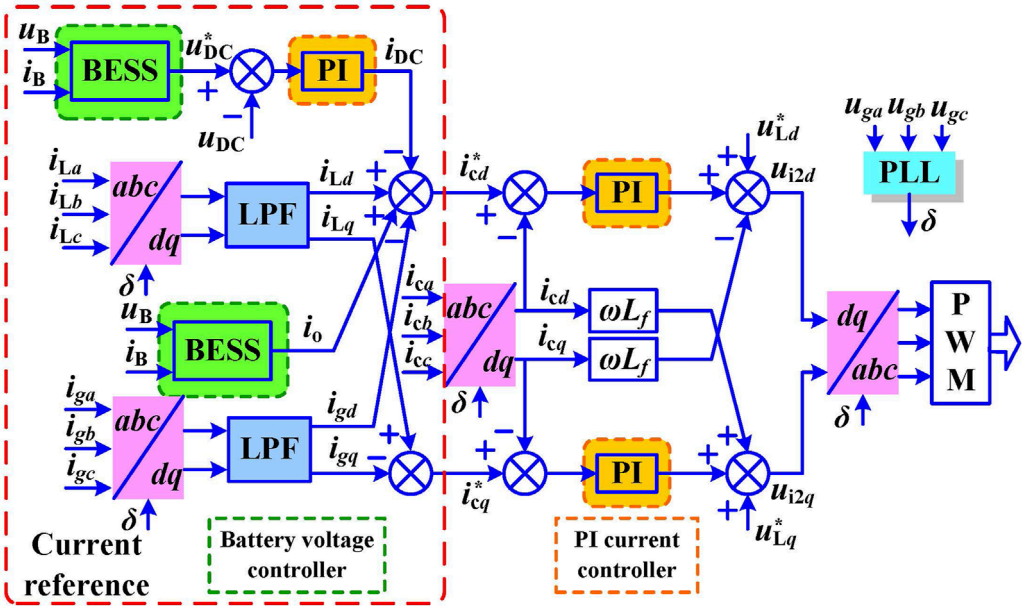

FIGURE 5
Control strategy of shunt converter.

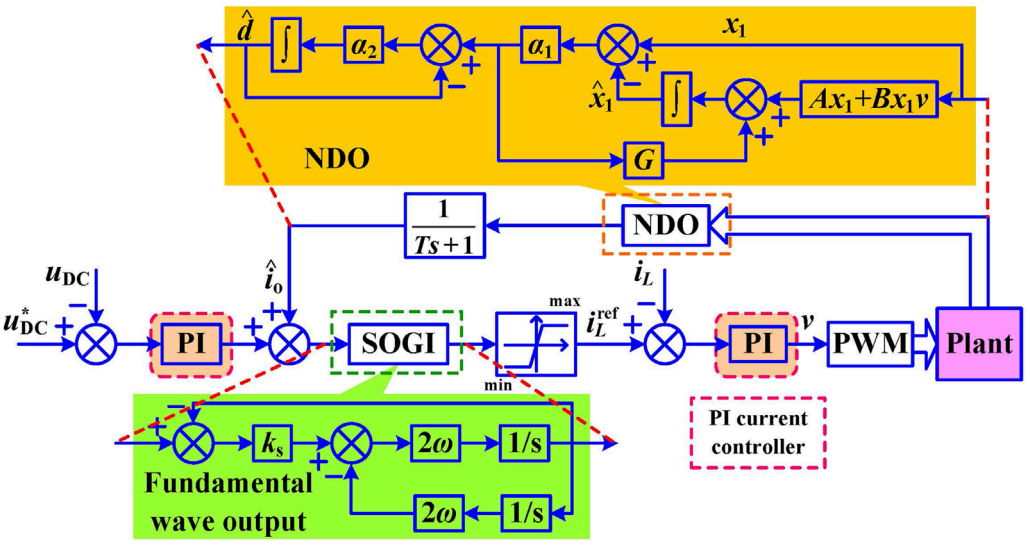

FIGURE 6
DC bus voltage control diagram of BESS.

to filter out high-frequency harmonics. The DC component in dq-axis can be expressed as

$$i_d = \frac{2}{3}\left[\cos\delta \quad \cos\left(\delta - \frac{2\pi}{3}\right) \quad \cos\left(\delta + \frac{2\pi}{3}\right)\right]\begin{bmatrix} i_a \\ i_b \\ i_c \end{bmatrix} \tag{22}$$

where δ is acquired by the phase-locked loop (PLL).

To realize bus voltage regulation and controller power balance, the compensation current reference is designed as

$$i_{cd}^{*} = i_{Ld} + i_o - i_{DC} - i_g \tag{23}$$

where i_{DC} represents the compensation signal generated by DC bus voltage deviation via PI controller. When the load does not vary, the signal i_{DC} provides power support for the system and compensates for power loss. i_{cq}^{*} is configured as zero.

TABLE 1 System parameters.

Parameter	Value
Grid voltage u_g	380 V
DC bus voltage reference u^*_{DC}	800 V
DC bus capacitor C_{DC}	2,200 μF
DC-DC converter inductor L_B	2 mH
Switching frequency f_s	10 kHz
PI controller of DC bus signal, k_{DCp}, k_{vDCi}	0.12, 0.55
PWM gains k_{pwm}	0.002
Bandwidth gain k_f	1
Observer gains α_1, α_2	−500, −2000
Inductor of series converter L_g	3 mH
Inductor of shunt converter L_f	2 mH
Cut-off frequency, ω_c	π rad/s
PI controller of shunt converter, k_{vp}, k_{vi}	0.001, 15
PI controller of series converter, k_{ip}, k_{ii}	0.021, 2.1
Q-PR controller gains, k_g, k_{gr}	0.2, 280.8
Switching frequency of inverter f_{sw}	20 kHz

To establish a unified control framework, the voltage control of the shunt converter is modified by adding the load voltage reference. The inner current control law is obtained as

$$\begin{cases} u_{i2d} = \left(k_{vp} + \dfrac{k_{vi}}{s}\right)\left(i^*_{cd} - i_{cd}\right) - \omega L_f i_{cq} + u^*_{Ld} \\ u_{i2q} = \left(k_{vp} + \dfrac{k_{vi}}{s}\right)\left(i^*_{cq} - i_{cq}\right) + \omega L_f i_{cd} + u^*_{Lq} \end{cases} \tag{24}$$

where k_{vp}, k_{vi} are the proportional and integral gains of the PI controller. The voltage signals (u_{i1d}, u_{i1q}, u_{i2d}, u_{i2q}) are yielded to implement the converter control.

3.3 BESS voltage controller design

Due to the power change and constant power characteristics at the load terminal, the current disturbance can affect the stability of DC bus voltage, especially in the case of drastic power change. Also, the BESS is connected with the converter, resulting in the existence of the double-frequency component in the current disturbance. The suppression of double-frequency ripple contributes to improving the output power quality and anti-interference performance of the BESS.

To suppress the fluctuation of DC bus voltage, an NDO-based voltage control approach is proposed in this paper. The DC bus voltage control approach of the BESS is displayed in Figure 6. The NDO is designed to achieve disturbance feedforward compensation and generate the disturbance estimate. The inductor current reference i^{ref}_L is produced by adding the current disturbance estimate $\hat{i}_o$ to the deviation signal via the PI controller. The SOGI is employed to eliminate the double-frequency ripple component of the current signal.

According to Equation 3, the state-space equation of the BESS is obtained as

$$\underbrace{\begin{bmatrix} \dot{u}_{DC} \\ \dot{i}_L \end{bmatrix}}_{\dot{x}} = \underbrace{\begin{bmatrix} 0 & \frac{1}{C_{DC}} \\ -\frac{1}{L_B} & 0 \end{bmatrix}}_{A} \underbrace{\begin{bmatrix} u_{DC} \\ i_L \end{bmatrix}}_{x} + \underbrace{\begin{bmatrix} -\frac{1}{C_{DC}} \\ \frac{1}{L_B} \end{bmatrix}}_{B} \underbrace{\begin{bmatrix} u_{DC} \\ i_L \end{bmatrix}}_{x} \underbrace{[d_j]}_{v} + \underbrace{\begin{bmatrix} -\frac{1}{C_{DC}} \\ 0 \end{bmatrix}}_{G} \underbrace{[i_o]}_{\tilde{d}} + \underbrace{\begin{bmatrix} 0 \\ \frac{u_B}{L_B} \end{bmatrix}}_{\bar{\omega}} \tag{25}$$

where A, B, and G are coefficient matrices, v is the system input, $\tilde{d}$ is the current disturbance.

To realize accurate disturbance observation, the NDO is developed as

$$\begin{cases} h_1 = \alpha_1 (x_1 - \hat{x}_1) \\ \dot{\hat{x}}_1 = Ax + Bxv + Gh_1 \\ h_2 = \alpha_2 \left(h_1 - \hat{\tilde{d}}\right) \\ \dot{\hat{\tilde{d}}} = h_2 \end{cases} \tag{26}$$

where $\hat{x}_1$ and $\hat{\tilde{d}}$ are estimates of x_1 and $\tilde{d}$, α_1 and α_2 are NDO gains, h_1 and h_2 are auxiliary variables. The accurately estimated current disturbance is fed to the output of the voltage control loop, which suppresses the DC bus voltage fluctuation induced by current disturbance.

The SOGI is employed to filter out the double-frequency component in the current reference so that there is no double-frequency ripple in the output of the converter (Alcala et al., 2010). Considering the double-frequency feature of the output current, the transfer function of the SOGI is expressed as

$$G_d(s) = \frac{k_f \omega_d s}{s^2 + k_f \omega_d s + \omega_d^2} \tag{27}$$

where k_f is the bandwidth gain, $\omega_d = 4\pi f$ rad/s.

According to Figure 6, we have

$$\begin{aligned} u_{DC}(s) = {} & \frac{k_{pwm} G_u(s) G_d(s) G_c(s)}{Cs + k_{pwm} G_u(s) G_d(s) G_c(s)} u^*_{DC}(s) \\ & - \frac{1}{Cs + k_{pwm} G_u(s) G_d(s) G_c(s)} i_o(s) \\ & + \frac{k_{pwm} \omega_c G_d(s) G_c(s)}{Cs^2 + \Xi s + \Upsilon} \hat{i}_o(s) \end{aligned} \tag{28}$$

where $\Xi = C\omega_c + k_{pwm} G_u(s) G_d(s) G_c(s)$, $\Upsilon = k_{pwm} \omega_c \; G_u(s) G_d(s) G_c(s)$, G_u and G_c are the gains of voltage and current PI controller, ω_c is the cut-off frequency. It reveals that the DC bus voltage Equation 28 can precisely track its reference and the NDO Equation 26 can achieve disturbance compensation. It can be seen from Equation 28 that the proposed controller Equations 26–28 has both tracking performance and disturbance rejection property.

Remark 1: Voltage sags and swells are among the most common disturbances. Voltage sags and swells can result from short circuits,

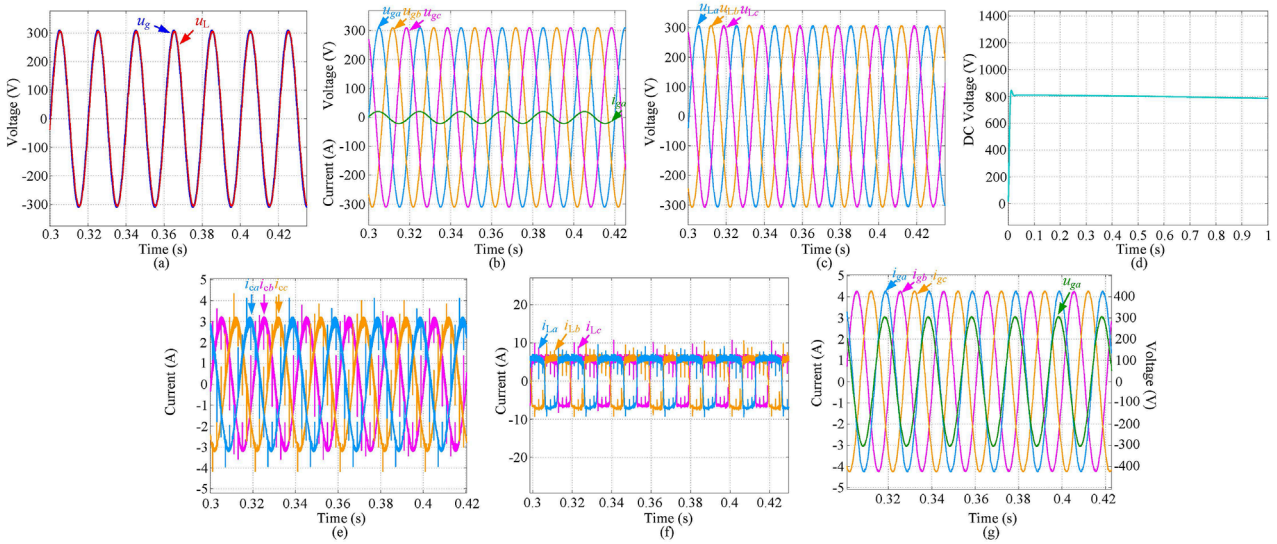

FIGURE 7
Dynamic results with nonlinear loads. **(A)** Grid voltage (u_g) and load voltage (u_L). **(B)** Grid voltages (u_{ga},u_{gb},u_{gc}) and grid current (i_{ga}). **(C)** Load voltage (u_{La},u_{Lb},u_{Lc}). **(D)** DC bus voltage (u_{DC}). **(E)** Compensation currents (i_{ca},i_{cb},i_{cc}). **(F)** Loads currents (i_{La},i_{Lb},i_{Lc}). **(G)** Grid currents (i_{ga},i_{gb},i_{gc}) and grid voltage (u_{ga}).

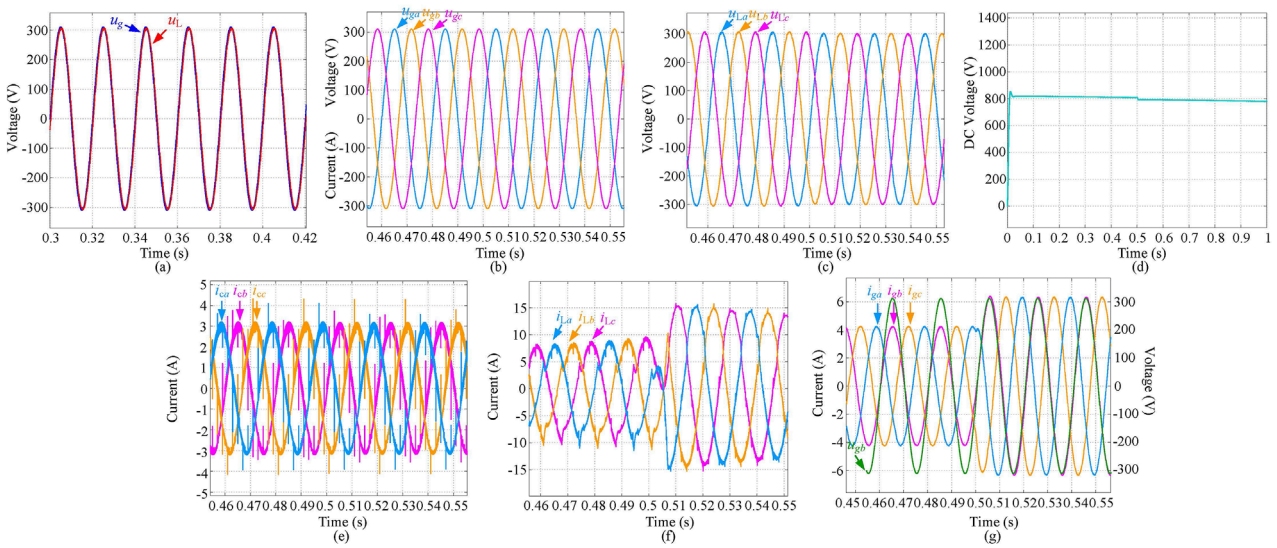

FIGURE 8
Dynamic results with load change. **(A)** Grid voltage (u_g) and load voltage (u_L). **(B)** Grid voltages (u_{ga},u_{gb},u_{gc}). **(C)** Load voltage (u_{La},u_{Lb},u_{Lc}). **(D)** DC bus voltage (u_{DC}). **(E)** Compensation currents (i_{ca},i_{cb},i_{cc}). **(F)** Loads currents (i_{La},i_{Lb},i_{Lc}). **(G)** Grid currents (i_{ga},i_{gb},i_{gc}) and grid voltage (u_{gb}).

large motor starts, or sudden changes in load (Somayajula and Crow, 2014). Since the presence of reactive power can cause inefficiencies in power delivery, the paper considers the ability of UPQC with BESS Equations 1–3, Equation 25 to provide reactive power compensation Equations 4–17. Also, the paper addresses disturbances caused by abrupt changes in load demand, which can affect both voltage stability and power quality. The proposed method can help in smoothing out these fluctuations Equations 18–24. In sum, in addition to current disturbances, a wide range of other disturbances are considered, including voltage sags, swells, and issues related to reactive power and load variations, which are mainly presented in the simulation cases.

4 Simulation results

The effectiveness of the voltage compensation control strategy is verified under different test conditions. The system model is

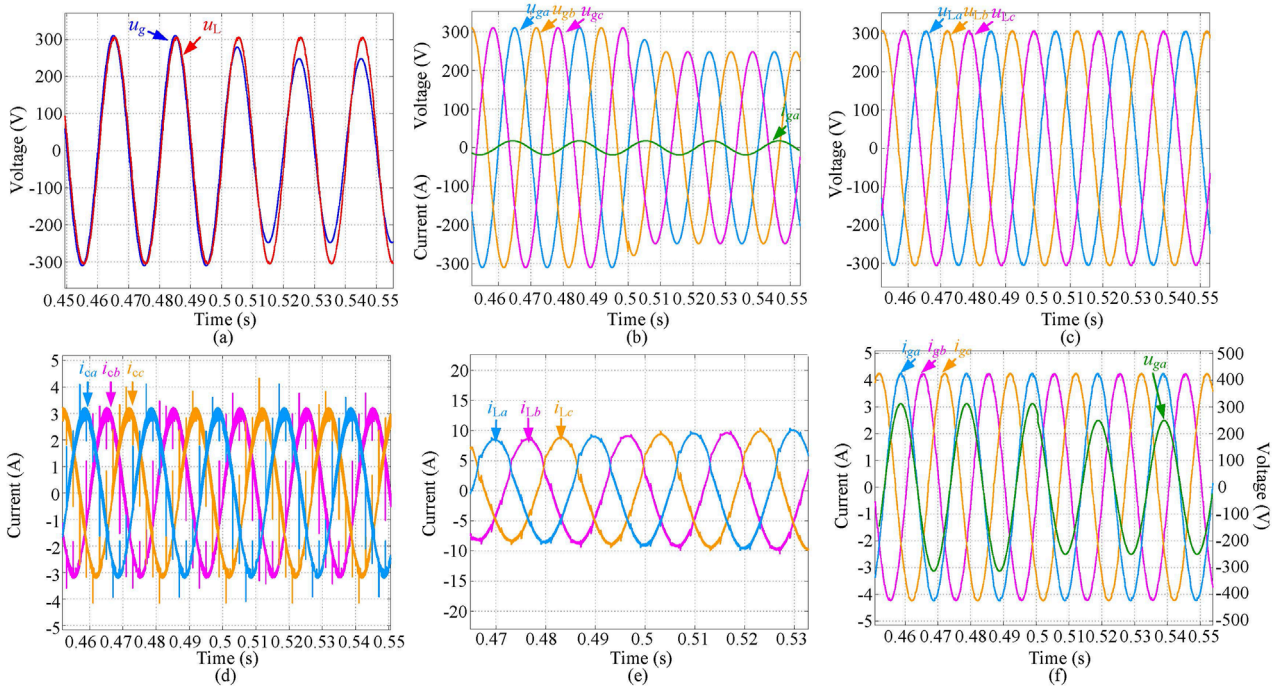

FIGURE 9
Dynamic results under voltage sag (20%). **(A)** Grid voltage (u_g) and load voltage (u_L). **(B)** Grid voltages (u_{ga},u_{gb},u_{gc}) and grid current (i_{ga}). **(C)** Load voltage (u_{La},u_{Lb},u_{Lc}). **(D)** Compensation currents (i_{ca},i_{cb},i_{cc}). **(E)** Loads currents (i_{La},i_{Lb},i_{Lc}). **(F)** Grid currents (i_{ga},i_{gb},i_{gc}) and grid voltage (u_{ga}).

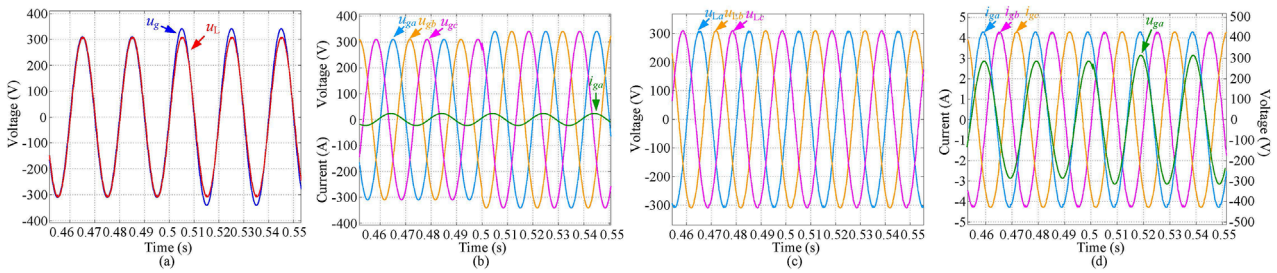

FIGURE 10
Dynamic results under voltage swell (10%). **(A)** Grid voltage (u_g) and load voltage (u_L). **(B)** Grid voltages (u_{ga},u_{gb},u_{gc}) and grid current (i_{ga}). **(C)** Load voltage (u_{La},u_{Lb},u_{Lc}). **(D)** Grid currents (i_{ga},i_{gb},i_{gc}) and grid voltage (u_{ga}).

built in the MATLAB/Simulink simulation environment. System parameters are presented in Table 1.

4.1 System performance with nonlinear loads

To verify the effectiveness of the proposed scheme, the nonlinear loads are applied to the system for the simulation test. The dynamic results of the UPQC with nonlinear loads are depicted in Figure 7. As shown in Figure 7A, the load voltage is 310.17 V. It can be seen that the proposed voltage compensation strategy achieves voltage vector compensation by the series converter. Figures 7B and G display the dynamic results of the grid voltages and grid currents. It is observed that the phase of the grid voltage is the same as that of the grid current. By the current compensation of the parallel converter, the output waveforms maintain smooth sinusoidal characteristics. Furthermore, the NDO guarantees the stabilization of the DC bus voltage under the condition of the current disturbance. It reveals that the proposed method realizes the comprehensive management of voltage quality and ensures the stability of DC bus voltage.

4.2 System performance with load change

To test the dynamic performance of the system, a simulation case is conducted considering load change. The dynamic results of the UPQC with load change are displayed in Figure 8. At $t = 0.5$ s, the load increases from 1000 W to 1500 W (0 → 500 Var). As observed in Figure 8A, the voltage vector can still be

compensated by the proposed control scheme under the condition of the load change. The compensation voltage generated by the series converter is injected into the system so that the grid voltage and the load voltage maintain in-phase sinusoidal characteristics. The compensation current generated by the parallel converter realizes the synchronization of the grid voltage and grid current. When the load increases, the load voltage can still remain constant with a satisfactory output effect, as shown in Figure 8C. It takes 13 ms to implement the quick response of the grid current. The results show that the proposed controller has a fast dynamic response and can ensure the smooth output of the grid current when the load changes instantaneously.

4.3 System performance under voltage sag and swell

Figures 9, 10 present the system dynamic results when the system encounters voltage sag and voltage swell. To validate the proposed control strategy, at $t = 0.5$ s, the grid voltage sag by 20% in Figure 9 and the grid voltage swell by 10% in Figure 10. It is obvious in Figures 9A, 10A that the amplitude-frequency characteristics of the grid voltage and load voltage are consistent when the system is operating normally. When the system fails, the amplitude of the grid voltage changes, but the phase of the grid voltage is still consistent with that of the load voltage. It can be noted that the proposed control scheme can still guarantee the smooth and stable output of grid voltage and current when the voltage sag or swell occurs. The UPQC with the proposed controller achieves the power quality improvement.

5 Conclusion

In this paper, a voltage compensation control strategy was proposed for the distribution network to achieve comprehensive management of power quality. To compensate for the amplitude and phase of the load voltage, a capacity configuration compensation scheme was proposed, which realizes the capacity configuration among parallel converter, series converter, and BESS. An NDO was designed to implement the current disturbance tracking and achieve disturbance compensation by a feedforward channel. Then, an NDO-based voltage control approach was developed for BESS to guarantee the stabilization of the DC bus voltage and improve the response speed of DC voltage. Simulation results demonstrated that the proposed control strategy effectively mitigated voltage sags and swells, significantly enhanced the dynamic response, and improved the overall stability and reliability of the distribution network, which highlighted the effectiveness of the integration of UPQC with BESS in managing power quality and enhancing system responsiveness. Future research will focus on robust cyber security measures to protect the grid from potential cyber threats and ensure the integrity of the control systems, combined with advanced control systems and energy storage technologies.

Data availability statement

The original contributions presented in the study are included in the article/supplementary material, further inquiries can be directed to the corresponding author.

Author contributions

YM: Writing–original draft, Writing–review and editing. JX: Writing–original draft, Writing–review and editing. CP: Writing–original draft, Writing–review and editing. WK: Writing–original draft, Writing–review and editing. GP: Writing–original draft, Writing–review and editing. GS: Writing–original draft, Writing–review and editing.

Funding

The author(s) declare that financial support was received for the research, authorship, and/or publication of this article. This work was supported in part by the Science and Technology Project of State Grid Xizang Electric Power Co., Ltd. (523101230003).

Conflict of interest

Authors YM, JX, CP, WK, GP, and GS were employed by Electric Power Research Institute of State Grid Xizang Electric Power Co., Ltd.

The authors declare that this study received funding from Electric Power Research Institute of State Grid Xizang Electric Power Co., Ltd. The funder had the following involvement in the study: collection, interpretation of data, the writing of this article, and the decision to submit it for publication.

Publisher's note

References

Abdalaal, R. M., and Ho, C. N. M. (2021). Analysis and validations of modularized distributed TL-UPQC systems with supervisory remote management system. *IEEE Trans. Smart Grid* 12 (3), 2638–2651. doi:10.1109/tsg.2020.3044992

Abdalaal, R. M., and Ho, C. N. M. (2022). System modeling and stability analysis of single-phase transformerless UPQC integrated input grid voltage regulation. *IEEE J. Emerg. Sel. Top. Power Electron.* 3 (3), 670–682. doi:10.1109/jestie.2021.3091395

Alcala, J. M., Castilla, M., De Vicuña, L. G., Miret, J., and Vasquez, J. C. (2010). Virtual impedance loop for droop-controlled single-phase parallel inverters using a second-order general-integrator scheme. *IEEE Trans. Power Electron.* 25 (12), 2993–3002. doi:10.1109/tpel.2010.2082003

Bacon, V. D., da Silva, S. A. O., and Guerrero, J. M. (2022). Multifunctional UPQC operating as an interface converter between hybrid AC-DC microgrids and utility grids, *Int. J. Electr. Power & Energy Syst.* 136 (3), 1–19. doi:10.1016/j.ijepes.2021.107638

Cardoso, J. T., Felinto, A. S., Jacobina, C. B., and Corrêa, M. B. d. R. (2024). Three-phase four-wire nine-leg AC-DC-AC converter based on high-frequency link. *IEEE Trans. Power Electron.* 39 (1), 885–897. doi:10.1109/tpel.2023.3327160

Carreno, A., Perez, M. A., and Malinowski, M. (2024). State-feedback control of a hybrid distribution transformer for power quality improvement of a distribution grid. *IEEE Trans. Ind. Electron.* 71 (2), 1147–1157. doi:10.1109/tie.2023.3262872

Çelik, D., and Ahmed, H. (2023). Enhanced control of superconducting magnetic energy storage integrated UPQC for power quality improvement in EV charging station. *J. Energy Storage* 62, 106843. doi:10.1016/j.est.2023.106843

Charalambous, A., Hadjidemetriou, L., Kyriakides, E., and Polycarpou, M. M. (2021). A coordinated voltage-frequency support scheme for storage systems connected to distribution grids. *IEEE Trans. Power Electron.* 36 (7), 8464–8475. doi:10.1109/tpel.2020.3046030

Dash, S. K., and Ray, P. K. (2021). A new PV-open-UPQC configuration for voltage sensitive loads utilizing novel adaptive controllers. *IEEE Trans. Ind. Inf.* 17 (1), 421–429. doi:10.1109/tii.2020.2986308

da Silva, S. A. O., Campanhol, L. B. G., Pelz, G. M., and de Souza, V. (2020). Comparative performance analysis involving a three-phase UPQC operating with conventional and dual/inverted power-line conditioning strategies. *IEEE Trans. Power Electron.* 35 (11), 11652–11665. doi:10.1109/tpel.2020.2985322

Devassy, S., and Singh, B. (2021). Performance analysis of solar PV array and battery integrated unified power quality conditioner for microgrid systems. *IEEE Trans. Ind. Electron.* 68 (5), 4027–4035. doi:10.1109/tie.2020.2984439

Felinto, A. S., Cunha, M. F., and Jacobina, C. B. (2022). Three-phase unified power quality conditioner based on high-frequency link. *IEEE Trans. Ind. Appl.* 58 (5), 6397–6407. doi:10.1109/tia.2022.3188599

Hosseini, M. M., and Parvania, M. (2023). Hierarchical intelligent operation of energy storage systems in power distribution grids. *IEEE Trans. Sustain. Energy* 14 (2), 741–750. doi:10.1109/tste.2022.3222425

Jin, T., Chen, Y., Guo, J., Wang, M., and Mohamed, M. A. (2020). An effective compensation control strategy for power quality enhancement of unified power quality conditioner. *Energy Rep.* 6, 2167–2179. doi:10.1016/j.egyr.2020.07.027

Khosravi, N., Echalih, S., Hekss, Z., Baghbanzadeh, R., Messaoudi, M., and Shahideipour, M. (2023). A new approach to enhance the operation of M-UPQC proportional-integral multiresonant controller based on the optimization methods for a stand-alone AC microgrid. *IEEE Trans. Power Electron.* 38 (3), 3765–3774. doi:10.1109/tpel.2022.3217964

Li, Z., Wu, L., Xu, Y., Wang, L., and Yang, N. (2023). Distributed tri-layer risk-averse stochastic game approach for energy trading among multi-energy microgrids. *Appl. Energy* 331, 120282. doi:10.1016/j.apenergy.2022.120282

Li, Z., Xu, Y., Wang, P., and Xiao, G. (2024). Restoration of a multi-energy distribution system with joint district network reconfiguration via distributed stochastic programming. *IEEE Trans. Smart Grid* 15 (3), 2667–2680. doi:10.1109/tsg.2023.3317780

Lou, G., Yang, Q., Gu, W., Quan, X., Guerrero, J., and Li, S. (2021). Analysis and design of hybrid harmonic suppression scheme for VSG considering nonlinear loads and distorted grid. *IEEE Trans. Energy Convers.* 36 (4), 3096–3107. doi:10.1109/tec.2021.3063607

Mahela, O. P., Khan, B., Alhelou, H. H., and Siano, P. (2020). Power quality assessment and event detection in distribution network with wind energy penetration using stockwell transform and fuzzy clustering. *IEEE Trans. Ind. Inf.* 16 (11), 6922–6932. doi:10.1109/tii.2020.2971709

Monteiro, V., Moreira, C., Lopes, J. A. P., Antunes, C. H., Osório, G. J., Catalão, J. P. S., et al. (2024). A novel three-phase multiobjective unified power quality conditioner. *IEEE Trans. Ind. Electron.* 71 (1), 59–70. doi:10.1109/tie.2023.3241380

Ray, P., Ray, P. K., and Dash, S. K. (2022). Power quality enhancement and power flow analysis of a PV integrated UPQC system in a distribution network. *IEEE Trans. Ind. Appl.* 58 (1), 201–211. doi:10.1109/tia.2021.3131404

Sanjenbam, C. D., Singh, B., and Shah, P. (2023). Reduced voltage sensors based upqc tied solar PV system enabling power quality improvement. *IEEE Trans. Energy Convers.* 38 (1), 392–403. doi:10.1109/tec.2022.3197408

Silva, S. A. O. D., Modesto, R. A., Sampaio, L. P., and Campanhol, L. B. G. (2024). Dynamic improvement of a UPQC system operating under grid voltage sag/swell disturbances. *IEEE Trans. Circuits Syst. II* 71 (5), 2844–2848. doi:10.1109/tcsii.2023.3263068

Somayajula, D., and Crow, M. L. (2014). An ultracapacitor integrated power conditioner for intermittency smoothing and improving power quality of distribution grid. *IEEE Trans. Sustain. Energy* 5 (4), 1145–1155. doi:10.1109/tste.2014.2334622

Song, G., Liu, X., Xiao, G., Chen, B., and Wang, P. (2024b). Decentralized adaptive control strategy of DC-DC boost converter for hybrid energy storage systems feeding CPLs. *IEEE J. Emerg. Sel. Top. Power Electron.* 12 (4), 3663–3674. doi:10.1109/jestpe.2024.3403000

Song, G., Liu, X., Xiao, G., Xiong, L., Chen, B., Wang, P., et al. (2024a). Circulating current suppression of power conversion systems under unbalanced conditions: large-signal model-based analysis. *CPSS Trans. Power Electron. Appl.* 9 (2), 152–165. doi:10.24295/cpsstpea.2023.00051

Tziovani, L., Hadjidemetriou, L., Kolios, P., Astolfi, A., Kyriakides, E., and Timotheou, S. (2022). Energy management and control of photovoltaic and storage systems in active distribution grids. *IEEE Trans. Power Syst.* 37 (3), 1956–1968. doi:10.1109/tpwrs.2021.3118785

Wang, H., Yan, Z., Shahidehpour, M., Zhou, Q., and Xu, X. (2021b). Optimal energy storage allocation for mitigating the unbalance in active distribution network via uncertainty quantification. *IEEE Trans. Sustain. Energy* 12 (1), 303–313. doi:10.1109/tste.2020.2992960

Wang, J., Sun, K., Wu, H., Zhu, J., Xing, Y., and Li, Y. (2021a). Hybrid connected unified power quality conditioner integrating distributed generation with reduced power capacity and enhanced conversion efficiency. *IEEE Trans. Ind. Electron.* 68 (12), 12340–12352. doi:10.1109/tie.2020.3040687

Xu, W., Zhu, W., and Shu, Z. (2023). Suppression of DC voltage ripple impact on non-isolated single-phase half-bridge unified power quality conditioner. *IEEE Trans. Ind. Electron.* 71, 10523–10532. doi:10.1109/TIE.2023.3337497

Yang, R., Jin, J., Zhou, Q., Mu, S., and Abu-Siada, A. (2022b). Superconducting magnetic energy storage based dc unified power quality conditioner with advanced dual control for DC-DFIG. *J. Mod. Power Syst. Clean. Energy* 10 (5), 1385–1400. doi:10.35833/mpce.2021.000354

Yang, R. H., and Jin, J. X. (2021). Unified power quality conditioner with advanced dual control for performance improvement of DFIG-based wind farm. *IEEE Trans. Sustain. Energy* 12 (1), 116–126. doi:10.1109/tste.2020.2985161

Yang, R. H., Jin, J. X., Mu, S., Zhang, M. S., Jiang, S., Chen, X. Y., et al. (2022a). Battery-energy-storage-based triple-active-bridge DC unified power quality conditioner for energy management and power quality enhancement of DC renewable sources, *Int. J. Electr. Power & Energy Syst.* 143 (4), 108442. doi:10.1016/j.ijepes.2022.108442

Zhang, R., Chen, Y., Li, Z., Jiang, T., and Li, X. (2024). Two-stage robust operation of electricity-gas-heat integrated multi-energy microgrids considering heterogeneous uncertainties. *Appl. Energy* 371, 123690. doi:10.1016/j.apenergy.2024.123690